Revista Mexicana de Física
ISSN: 0035-001X
rmf@ciencias.unam.mx
Sociedad Mexicana de Física A.C.
México

García-Ruiz, A.; Rodríguez-Mora, J.I.; Morales, A.; Aguilar, M.; Zorrilla, C.; Ascencio, J.A.
Structural determination and Rietveld refinement of BaX TiY OZ subspecies
Revista Mexicana de Física, vol. 55, núm. 1, 2009, pp. 52-56
Sociedad Mexicana de Física A.C.
Distrito Federal, México

Structural determination and Rietveld refinement of $Ba_XTi_YO_Z$ subspecies

A. García-Ruiz
Unidad Profesional Interdisciplinaria de Ingeniería y Ciencias Sociales y Administrativas-COFAA, Instituto Politécnico Nacional, Te 950, Col. Granjas-México, 08400 México, D.F., Mexico, e-mail: amado.garcia@gmail.com

J.I. Rodríguez-Mora
Instituto de Física, Universidad Autónoma de Puebla, Apartado Postal J-48, Puebla, 72570, México.

A. Morales, M. Aguilar, and C. Zorrilla
Instituto de Física, Universidad Nacional Autonóma de México, México, D.F., Mexico.

J.A. Ascencio
Instituto de Ciencias Físicas, Universidad Nacional Autonóma de México, Av. Universidad s/n, Col. Chamilpa, Cuernavaca, Mexico.

Recibido el 23 de agosto de 2008; aceptado el 8 de diciembre de 2008

Multiple works have been reported about the synthesis of $Ba_xTi_yO_z$, that allows a piezoelectric behavior, however the determination of the structure is no simple and consequently it requires a deeper analysis. In our case we are obtaining systems with arrays of small crystals (around 50 nm), producing bigger structures with channels and high superficial area value. The capability of the material to keep no central atom unit cells becomes indispensable and critical for the piezoelectric proposes. The size and the crystalline structure are studied by using electron microscopy techniques, particularly scanning for the configuration analysis, and transmission techniques to get the size of the structural domains, besides the nanometric characterization. X-ray diffraction and Rietveld refinement methods were used to determine the crystalline phases present in the produced samples for a whole characterization.

Keywords: Nanoparticles; Barium titanate; Rietveld refinement; electron microscopy.

Muchos trabajos han sido reportados acerca de la síntesis de $Ba_xTi_yO_z$, que permite un comportamiento piezoeléctrico, sin embargo la determinación de la estructura asociada no es simple y consecuentemente ella requiere de un análisis más profundo. En nuestro caso estamos obteniendo sistemas con arreglos de pequeños cristales (alrededor de 50 nm), produciendo estructuras más grandes con canales y alto valor de área superficial. La capacidad de contar con celdas unitarias sin átomo central es indispensable y crítica para propósitos piezoeléctricos. El tamaño y la estructura cristalina son estudiados por técnicas de microscopía electrónica, particularmente barrido para el análisis de configuraciones, y transmisión para obtener el tamaño de los dominios estructurales, como alternativa a la caracterización nanométrica. Métodos de difracción de rayos X y refinamiento Rietveld fueron usados para determinar las fases cristalinas presentes en las muestras producidas para una plena caracterización.

Descriptores: Nanopartículas; titanato de Bario; refinamiento Rietveld; microscopía electrónica.

PACS: 65.80.+n; 82.60.Qr; 61.05.C; 68.37.Ef; 68.37.Lp.

1. Introduction

Many works have been reported about the synthesis of $Ba_xTi_yO_z$. This is because the different species of barium titanate have shown very important properties such as ferroelectricity and piezoelectricity; the $BaTi_2O_5$ and $BaTiO_3$ phases are two of them, which show very notables piezoelectric, optical and electrochemical properties especially when the size of the crystallites is in the nanometric scale. There are several synthesis methods which have been used with more or less success in order to obtain $BaTiO_3$ [1-3]. The obtained subspecie depends on the relation Ba:Ti in the precursors and on the preparation conditions. The $BaTiO_3$ subespecie has shown porous structures which could be utilized for the transport and dosage of drugs or medicines in zones where there is an increment of pressure (inflammation or reduction of blood vessels). Also it could be applied in the fabrication of data storages or mechanical and chemical sensors.

In order to contribute to the obtaining of this kind of materials, in this work assays are reported to prepare divers subspecies of titanate using a synthesis method based on the decomposition of bimetallic alcoxides. The general aim of this work is to prepare samples with pure subspecies of barium titanates, especially $BaTiO_3$ and to make a good characterization in all properties of the samples. The particular aim is to make the structural characterization using X-ray diffraction and Rietveld refinements. Also here, it is presented SEM images which show the basic morphology of these materials. These samples were characterized mainly for running their

TABLE I. Phase's concentration (wt%) in the whole diffraction patterns. For IP1-2, two possible refinements are shown.

Sample	$BaTi_2O_5$ Monoclinic	$BaTiO_3$ Tetragonal	$Ba_4Ti_{13}O_{30}$ Orthorhombic
IP1-1	91.2 (9)	4.2 (1)	4.6 (3)
IP1-2 (1Ph)	100 (2)		
(2Ph)	98.3 (8)		1.7 (2)

TABLE II. Lattice parameters of the major phase, $BaTi_2O_5$ Monoclinic, in both samples.

Sample	a (nm)	b (nm)	c (nm)	β(degrees)
IP1-1	1.69070 (3)	0.393009 (7)	0.94403 (2)	103.0541 (7)
IP1-2 (1Ph)	1.69086 (4)	0.392651 (9)	0.94514 (2)	103.036 (1)
(2Ph)	1.69083 (4)	0.392648 (9)	0.94511 (2)	103.035 (1)

TABLE III. Average crystallite size of the Monoclinic Phase $BaTi_2O_5$

Sample	Average crystallite size $BaTi_2O_5$ Monoclinic (nm)
IP1-1	90.8 (2)
IP1-2 (1Ph)	79.3 (3)
(2Ph)	79.4 (3)

X-ray diffraction patterns with a good statistic in order to refine the pattern and to calculate the phase concentrations.

Conditions of preparation and thermal treatment are related with the phase concentration and the crystal size. The refinement of the crystalline phases by using the Rietveld method provided the phase concentrations (wt%) for all the identified phases: $BaTi_2O_5$ Monoclinic, $BaTiO_3$ Tetragonal and $Ba_4Ti_{13}O_{30}$ Orthorhombic.

2. Experimental methods

Samples were prepared by a synthesis method based on the decomposition of bimetallic alcoxides. In this synthesis, stechiometric amounts of barium isopropoxide and titanium isopropoxide, with Ba:Ti ratio of 1:1, 1:2 and 1:3 were aggregated to isopropanol. This solution was kept under stirring until it takes a yellow color not translucent (milky). Then, the milky solution was dried for obtaining a clear yellow powder. Oxidation of this powder was got by means a thermal treatment at temperatures of 300, 600, and 900°C by 3 hours in order to eliminate organic residues and to increase the amount of the ceramic material. To control the morphology, different amounts of heptadecane and oleic acid were used before calcination procedure.

Morphology of the samples was observed in JEOL 5400LV scanning electronic microscope (SEM), which has also analytical system for chemical composition studies. The low vacuum mechanism allows a no sample preparation, considering just the deposition of the material on the sample holder. A JEOL field emission transmission electron microscope (with 200 keV) was used to obtain high resolution transmission electron micrographs; in order to prepare a sample for this analysis, we put a drop on a cupper grid, so we selected the best conditions for observation using the contrast transfer function and Scherzer condition for optimum defocus (Δf$\sim$30.2 nm for the used microscope). The X-ray powder diffraction pattern of the sample packed in a glass holder was recorded at room temperature with CuK_α radiation in a Bruker Advance D-8 diffractometer that had a θ–θ configuration and a graphite monochromator in the secondary beam. Diffraction intensity was measured between 10 and 110°, with a 2 θ step of 0.02° for 4.0 s per point. Sample was 1.5 mm thick. Crystalline structures were refined with the Rietveld technique by using FULLPROF98 code [4]; peak profiles modeled with pseudo-Voigt functions [5] contained a refinable parameter related with average crystallite size for every phase [6]; the reliability of those parameters is discussed in detail elsewhere. The effect of the average crystallite size was included in the Lorentzian part of the function. The standard deviations of the refined parameters are not estimates of the probable error in the analysis as a whole, but only of the minimum possible probable errors based on their normal distribution [7]. A maximum of seventy one variables, when the identified phases were three, were refined including, for every phase, the scale factor, the refinable atom fractional coordinates, the lattice parameters, the isotropic thermal displacements and the crystallite size parameter. The quality of the refinement (of the fitting) is measured by a residual function Rwp.

3. Results and discussion

Because the kind of possible applications, we tried to get the best conditions to produce structures with channels and we are reporting here the considered as the optimum. Samples with Ba:Ti ratio of 1:2, were labeled as IP1-1 and IP1-2. IP1-1 was dissolved in heptadecane with oleic acid as surfactant and treated at 900°C, while IP1-2 does not consider the use of the surfactant.

The analysis of these samples can be observed in Fig. 1, where several micrographs obtained by using the SEM can be observed. Considering the images obtained at 7500 and 15000 magnifications (Figs. 1a and 1b) for sample IP-1, the identified aggregates are homogeneous channels morphologies with porous of 20 to 40 nm. For sample IP-2, much bigger morphologies can be distinguished, produced by bigger holes (Fig. 1c) observed at 500X, which denotes structures with diameter up to 150μm, instead the materials with diameters of 5μm of the previously mentioned clusters; the micrograph of Fig. 1d, which corresponds to a major magnification (15000X) allowed to determine that the porous of about 0.5 to 2 μm are formed by multiple smaller particles (these figures show examples but multiple micrographs were studied

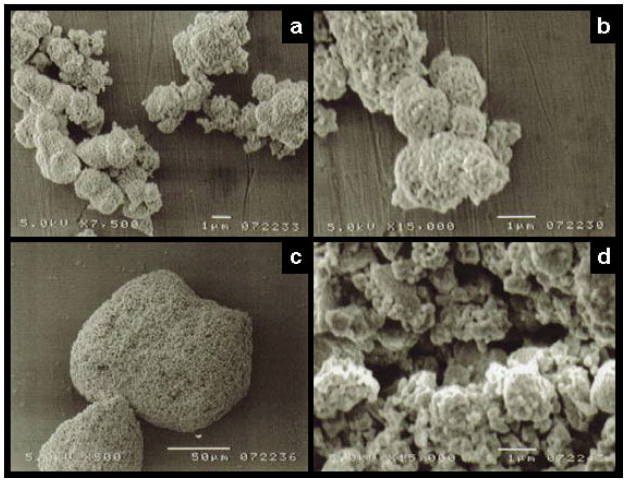

FIGURE 1. SEM images of two different regions of each sample, observed at a) 7500X and b) 15000X magnifications, for IP-1; besides c) 500X and d) 15000X magnifications for IP-2. Images denote different behavior of the material, but in both cases the sponge like morphology is clear.

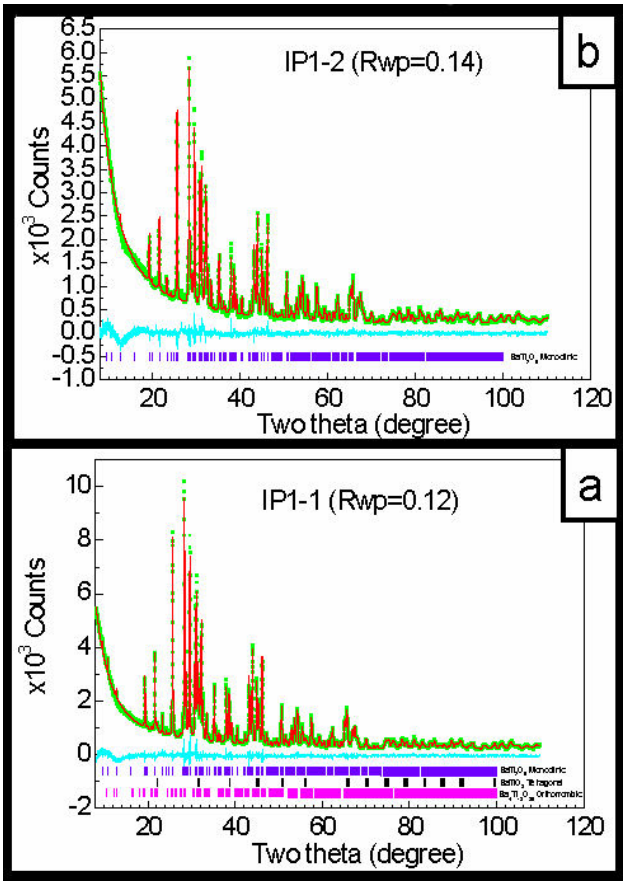

FIGURE 2. Typical refinement modeled with a) three phases or subspecies of barium titanate in the sample IP1-1. Upper marks are the $BaTi_2O_5$ reflections, middle marks are the $BaTiO_3$, and lower marks are the $Ba_4Ti_{13}O_{30}$ ones and b) single phase of $BaTi_2O_5$. Experimental pattern is denoted by symbols and the refined one is in continuous line.

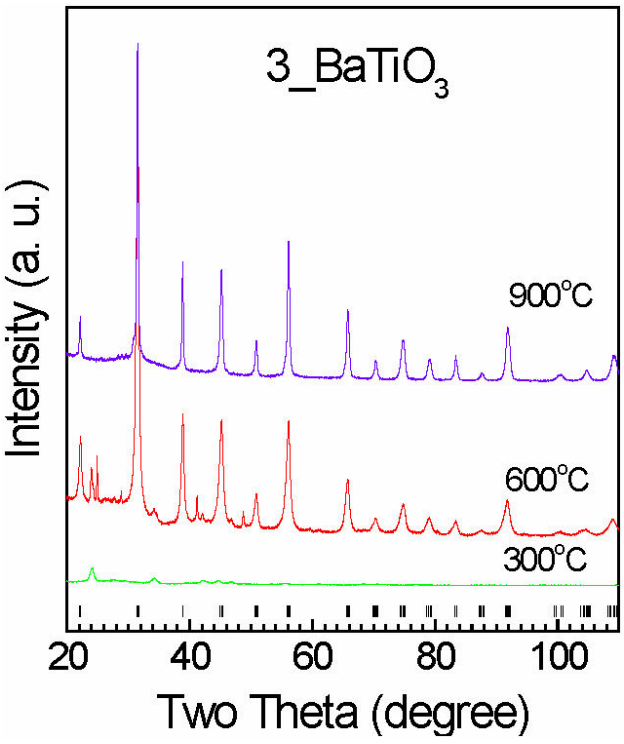

FIGURE 3. Graphic arrangement of patterns showing that the synthesis method is useful to prepare (at 900°C) pure titanate $BaTiO_3$ (marks).

to clarify this dimension and the channels). From both samples it is possible corroborate that the morphology is a sponge type with a high porous density. This feature suggests that the material owns also a very high superficial area in comparison with bulk material assuring a high reactivity to retain a suitable stuffing material; but also it suggests that the conformation of samples involves more than one single phase. In this way it is indispensable to increase the information about the material; we used X-ray diffraction and TEM analysis to determine the crystalline phases.

The use of X-ray diffraction analysis is implemented besides the application of Rietveld refining method in order to determine the present phases and the own parameters of them. In this way, Fig. 2 shows the two different samples studied also by SEM; in the figures, by means the use of typical refinement, modeled patterns are established besides the experimental data. For the first case of Fig. 2a (that corresponds to the small aggregates of Fig. 1a), upper marks are the $BaTi_2O_5$ reflections, middle marks are the $BaTiO_3$, and lower marks are the $Ba_4Ti_{13}O_{30}$ ones; while Fig. 2b obtained for the sample with bigger aggregates (Fig. 1b) the evidence is of just one phase, $BaTi_2O_5$ whose reflections are presented with marks. The quality of the refinements is shown graphically by the difference between both patterns which appears as the lowest and noisily continuous line, also is given by Rwp = 0.12 and 0.14 respectively.

For refining, for the $BaTi_2O_5$Monoclinic phase, the structure was modeled using a unit cell with a symmetry given by the space group C_12_1 (S.G. 5). For the $BaTiO_3$ Tetragonal the

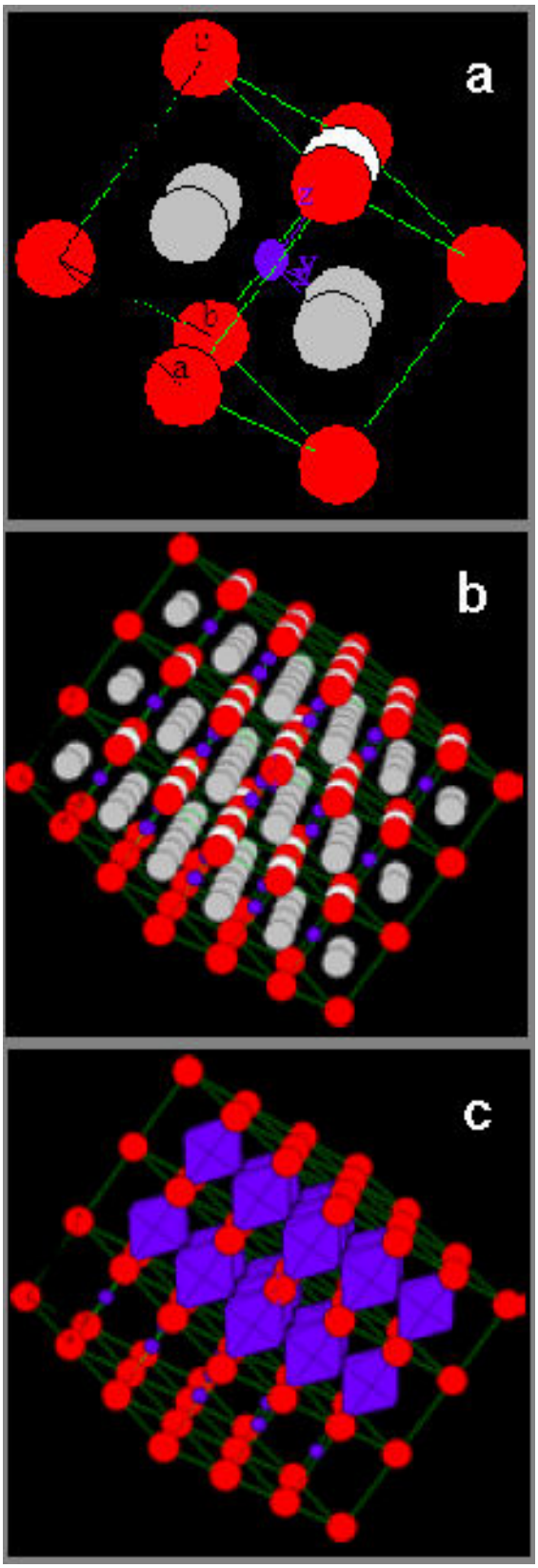

FIGURE 4. Derived models of a) the tetragonal cell corresponding to the nanocrystalline $BaTiO_3$. a=b=0.4005nm, c=0.4038 nm b) a small lattice, and c) the small lattice showing some octahedrons formed around the titanium atom. Ba (red), Ti (blue), O (white/gray)

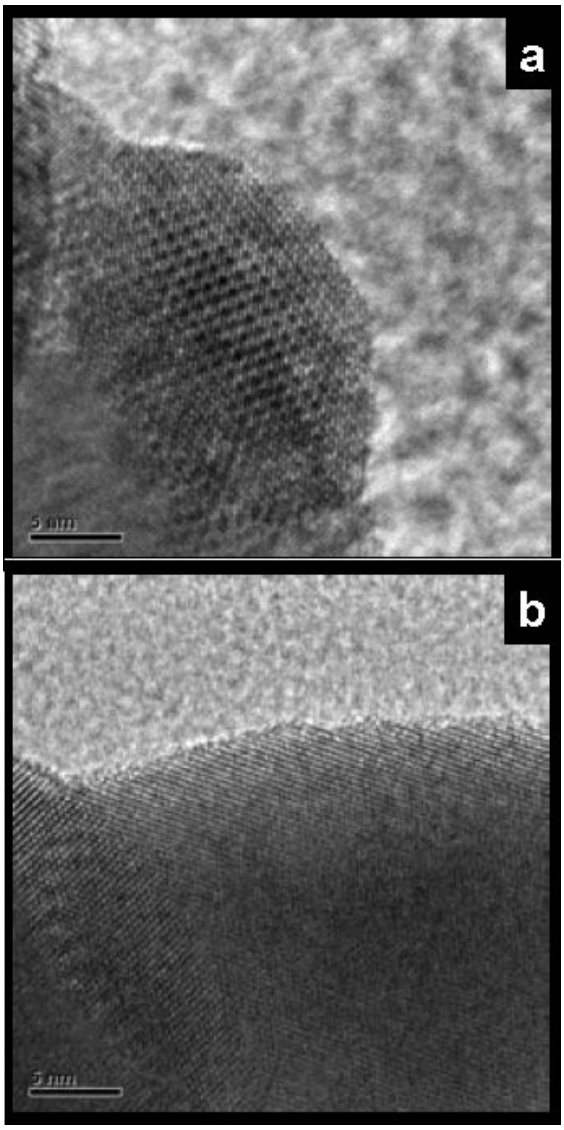

FIGURE 5. TEM images of samples a) IP-1 and b) IP-2, where high resolution is clear and the presence of clusters of different sizes too.

symmetry used for the unit cell was that of the space group *P4mm* (S.G. 99). Finally, for the $Ba_4Ti_{13}O_{30}$ Orthorhombic the symmetry used for the unit cell was that of the space group *Cmca* (S.G. 64). In all cases, with the initial atom positions obtained from the literature [8-10].

Table I shows the contribution of every phase in the whole diffraction patterns. Sample IP1-1 showed the three different subspecies with the phase $BaTi_2O_5$ as a major phase; the concentration of this phase was 91.2%. Sample IP1-2 was refined with just a phase $BaTi_2O_5$; however, the refinement was improved when a second phase was added obtaining just a 1.7% of this second phase. That means that in this sample the phase $BaTi_2O_5$ is almost pure, into a margin of 1 or 2% of error.

In Table II, it is reported the result of the refined lattice parameters for the major phase $BaTi_2O_5$, present in the two samples. They were started from similar values reported in

the literature cited above. In the sample IP1-2, the presence of a second phase does not change in an important manner the values of the parameters.

In Table III, it is reported the nanometric size of the crystallites only for the main phase $BaTi_2O_5$. Here is possible to observe that the crystallites in IP1-1 are bigger than the crystallites for the sample IP1-2, but that the crystallite size is almost not affected by the presence of the second phase. In any case, for the two samples the average crystallite size for the major phase is reported, finding that the crystallites are between 50 and 100 nm in these samples. In $BaTiO_3$, only the coordinates z for Ti and O atoms were refined; x and y are fix coordinates in its symmetry. However, we must remember that even when the X-ray study derivates into these average values, the scanning electron micrographs involve the presence of smaller clusters for the sample IP-1 and a deeper analysis is important for discriminating this behavior.

Finally, it is convenient to show some preliminary results in order to get the synthesis of the pure nanophase $BaTiO_3$. Figure 3 shows an arrangement of successive diffraction patterns to illustrate graphically the used process to arrive to the pure titanate $BaTiO_3$: after the preparation of the titanate powder it is necessary to give to the material a thermal treatment up to 900°C. The refinement of this series of samples is in process.

Anyway, starting from the results of the refinement of the phase $BaTiO_3$ of the sample IP1-1, it was possible to generate a unit cell model of the correspondent crystallite of tetragonal geometry and a small crystal; in the Fig. 4 the results are shown. The corresponding symmetry and atomic distribution is associated to the own properties of the materials and particularly for the use in devices where piezoelectric properties are important, the no central atom is a condition and the size of the aggregates.

In order to determine directly the way that material is aggregated, TEM micrographs are used for each sample and consequently we can confirm the lowest magnification evidences. In this way, selected images allow to identify the presence of clusters around 30 nm on the surface of sample IP-1 (Fig. 5a), while for sample IP-2 (Fig. 5b) the crystalline structures are bigger than 100 nm. The presence of smaller clusters involves the possibility to generate smaller porous too; because the same dimension, the higher curvature can be associated to the observed morphologies by SEM. We must also remember this to understand the properties of the produced materials, for catalytic mechanisms and also for the capability of the sponge-like structure for piezoelectric applications.

4. Conclusions

It has been demonstrated that the utilized synthesis method is successful to obtain the different subspecies of barium titanate. The samples prepared and analyzed, depending of the conditions of treatment, showed the presence of the two phases with more interest in a concentration next to the pure phase. The features showed in the SEM images make sure that these materials have a sponge-type morphology whit an high porosity, for which this material should be very convenient to become a good receptacle to liberate in a controlled manner drugs or medicines in zones where the local pressure and its changes allow the control. It is also demonstrated that the different samples induce different size clusters on the surface of the materials, deriving into a variation of the morphology, the porous formation and the consequent catalytic and piezoelectric properties. The application of both microscopy and diffraction methods, with the Rietveld refinement allowed a whole characterization of our samples and open the selection of synthesis conditions for improving the formation of a particular phase and consequently possible application.

1. Ch. Pithan, D. Hennings, and R. Waser *Int. J. Appl. Ceram. Technol* **2** (2005) 1.
2. K.W. Kirby, *Mat. Res. Bull* **23** (1988) 881.
3. W.S. Yun, J.J. Urban, Q. Gu, and H. Park, *Nano Lett* **2** (2002) 447.
4. J. Rodríguez-Carbajal, *Laboratoire Leon Brillouin* (CEA-CNRS), (France Tel: (33) 1 6908 3343, Fax: (33) 1 6908 8261, e-mail: juan@llb.saclay.cea.fr).
5. P. Thompson, D.E. Cox, and J.B. Hasting, *J. Appl. Crystallogr.* **20** (1987) 79.
6. R.A. Young and P. Desai, *Arch. Nauki Mater.* **10** (1989) 71.
7. E. Prince, *J. Appl. Crystallogr.* **14** (1981) 157.
8. T. Kimura *et al.*, *Acta Crystallographica C* **59** (2003) 128.
9. G. H. Kwei, A. C. Lawson, jr., S. J. L. Billinge, and S.-W. Cheong, *Journal of Physical Chemistry* **97** (1993) 2368.
10. E. Tillmanns, *Crystal Structure Communications* **11** (1982) 2087.